Supporting information

Constructing {Co^{II}_6} hexagon-centered heterometallic {Ln_6Co_6} (Ln = Y, Eu and Dy) clusters with calix[8]arene ligand

HaitaoHan[I,ac] You-Song Ding[I,b] XiaofeiZhu,[a] Tian Han,[b] Yan-Zhen Zheng*[b] and Wuping Liao*[a]

[a]State Key Laboratory of Rare Earth Resource Utilization, Changchun Institute of Applied Chemistry, Chinese Academy of Sciences, Changchun 130022, China
[b]Frontier Institute of Science and Technology (FIST), State Key Laboratory of Mechanical Behavior of Materials and MOE Key Laboratory for Nonequilibrium Synthesis and Modulation of Condensed Matter, Xi'an Jiaotong University, Xi'an 710054, China
[c]University of Chinese Academy of Sciences, Beijing 100049, China

Table S1 Crystal data and structure refinement for compounds **CIAC-248--250**.

	CIAC-248	**CIAC-249**	**CIAC-250**
formula	$C_{301.35}H_{412.30}Co_6N_7O_{48.30}Y_6$	$C_{301}H_{409}Co_6Eu_6N_7O_{47}$	$C_{302}H_{415}Co_6Dy_6N_7O_{49}$
formula wt	5792.75	6142.67	6255.97
cryst. syst.		monoclinic	
space group		*C2/c*	
a (Å)	59.2342(13)	59.4388(14)	59.484(2)
b (Å)	33.8392(7)	33.8457(8)	34.0418(9)
c (Å)	42.2121(9)	42.4684(18)	42.7405(14)
α (°)	90	90	90
β (°)	126.210(10)	125.999(1)	125.883(3)
γ (°)	120	90	90
V(Å^3)	68269(3)	69120(4)	70117(4)
Z		8	
D_c/g cm^{-3}	1.128	1.181	1.185
μ / mm^{-1}	4.008	10.315	9.334
F(000)	24415	25440	25808
total data	47833	23928	31891
unique data	40082	18897	27462
GOF	1.040	1.033	1.043
R_1[a] [I > 2σ(I)]	0.0975	0.0806	0.0796
wR_2[b](all data)	0.2951	0.2331	0.2302

[a]$R_1 = \Sigma||F_0|-|F_c||/\Sigma|F_0|$; [b]$wR_2 = \{\Sigma[w(F_0^2-F_c^2)^2]/\Sigma[w(F_0^2)^2]\}^{1/2}$

Table S2 Continuous Shape Measures calculation of the coordination geometry for Dy(III) ions in Co_6Dy_6

Structure [ML7]	HP-7	HPY-7	PBPY-7	**COC-7**	**CTPR-7**	JPBPY-7	JETPY-7
Dy1	32.743	18.909	4.689	**1.775**,	1.910	8.035	20.315
Dy2	33.496	19.088	4.765	1.729	**1.471**	8.282	20.766
Dy5	34.032	19.819	4.971	3.684	**2.589**	7.907	20.346
Dy4	33.195	19.023	4.694	1.818	**1.705**	8.001	21.254

HP-7	1	D7h	Heptagon
HPY-7	2	C6v	Hexagonal pyramid
PBPY-7	3	D5h	Pentagonal bipyramid
COC-7	**4**	**C3v**	**Capped octahedron**
CTPR-7	**5**	**C2v**	**Capped trigonal prism**
JPBPY-7	6	D5h	Johnson pentagonal bipyramid J13
JETPY-7	7	C3v	Johnson elongated triangular pyramid J7

Structure [ML8]	OP-8	HPY-8	HBPY-8	CU-8	SAPR-8	TDD-8	JGBF-8	JETBPY-8	**JBTPR-8**	BTPR-8	SD-8	TT-8	ETBPY-8
Dy6	31.747	20.522	11.923	10.089	4.143	4.109	10.142	22.949	**2.461**	2.813	4.142	10.313	21.889
Dy3	28.604	20.485	13.556	10.448	2.429	2.617	11.935	23.610	**2.137**	2.334	3.111	11.032	23.027

OP-8	1	D8h	Octagon
HPY-8	2	C7v	Heptagonal pyramid
HBPY-8	3	D6h	Hexagonal bipyramid
CU-8	4	Oh	Cube
SAPR-8	5	D4d	Square antiprism
TDD-8	6	D2d	Triangular dodecahedron
JGBF-8	7	D2d	Johnson gyrobifastigium J26
JETBPY-8	8	D3h	Johnson elongated triangular bipyramid J14
JBTPR-8	**9**	**C2v**	**Biaugmented trigonal prism J50**
BTPR-8	10	C2v	Biaugmented trigonal prism
JSD-8	11	D2d	Snub diphenoid J84
TT-8	12	Td	Triakis tetrahedron
ETBPY-8	13	D3h	Elongated trigonal bipyramid

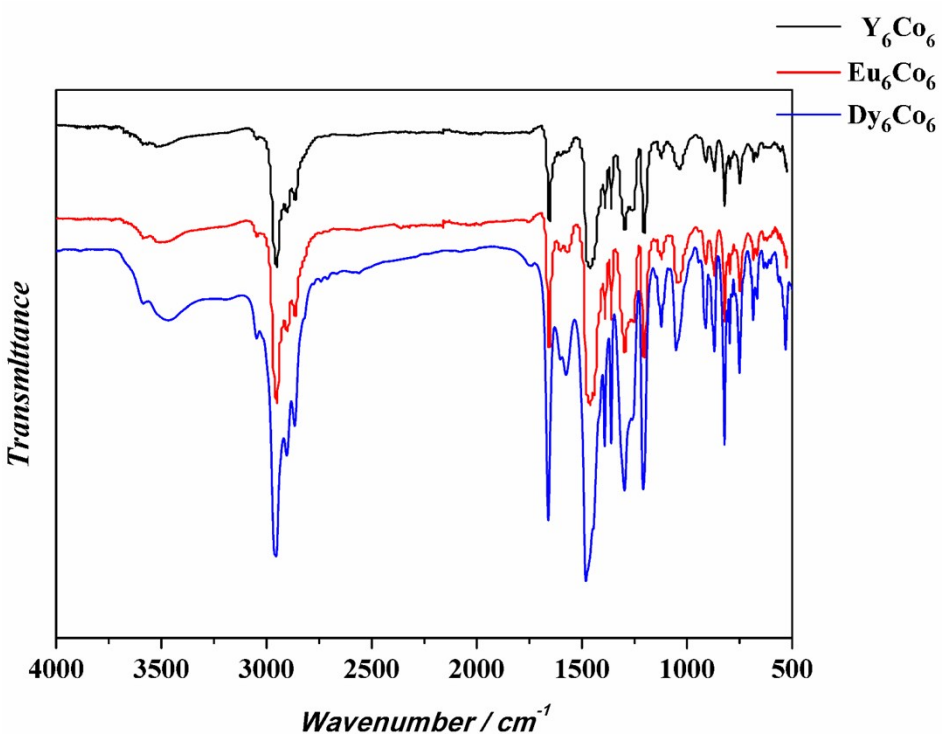

Fig.S1 FT-IR spectra for compounds **CIAC-248--250**.

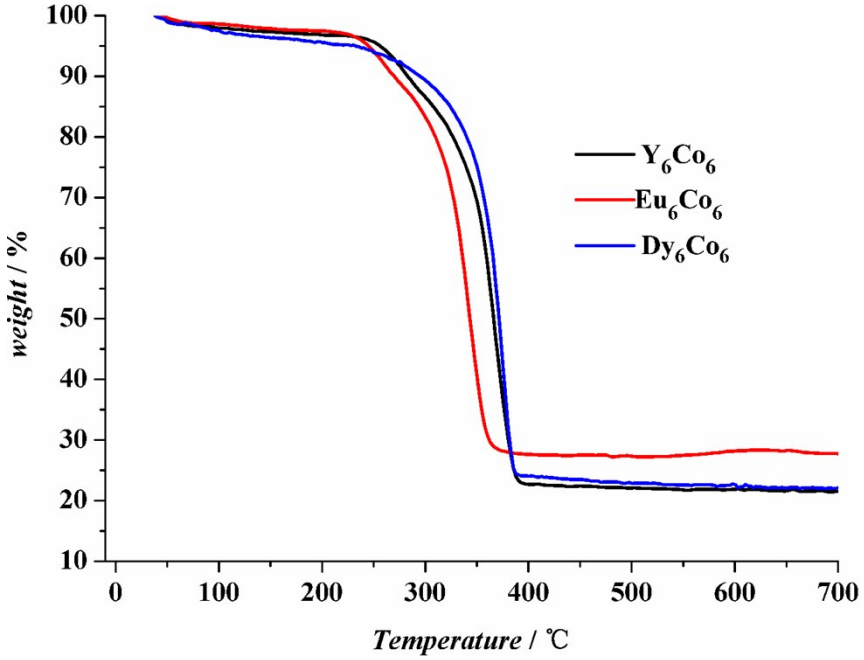

Fig.S2 TG curves for compounds **CIAC-248--250.**

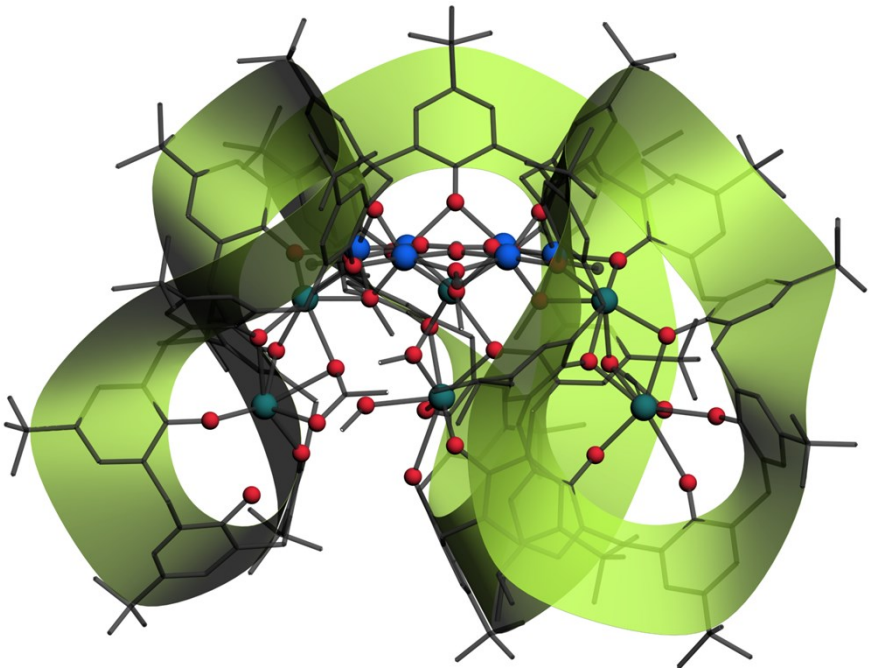

Fig.S3 Side view of Compound **CIAC-250**.

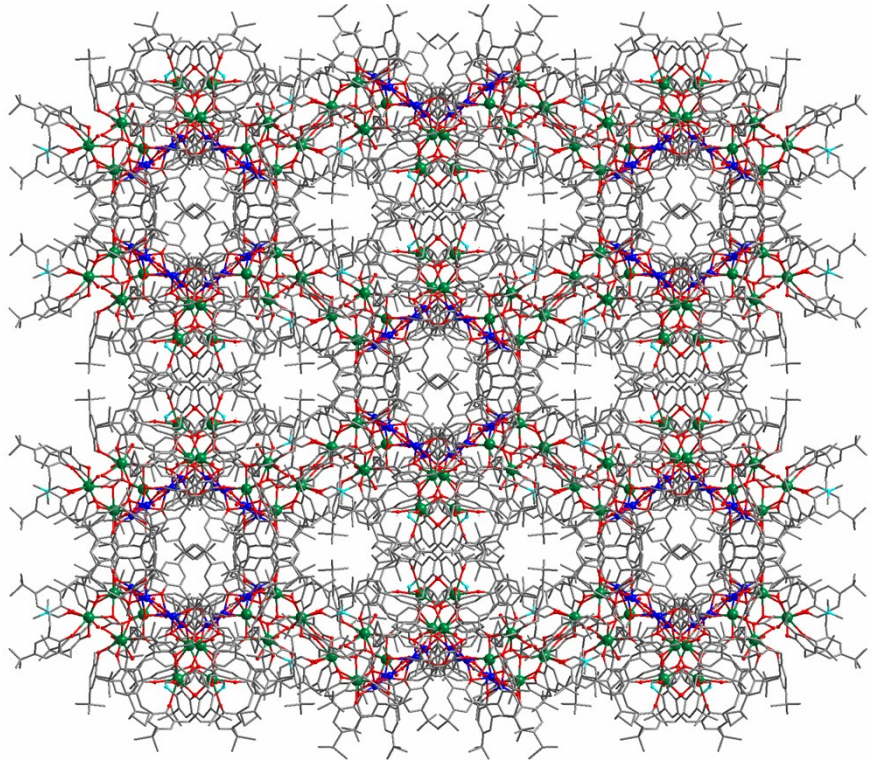

Fig.S4 Supramolecular extended structure of **CIAC-250**. Solvent molecules are omitted for clarity. Blue: Co; Green: Ln.

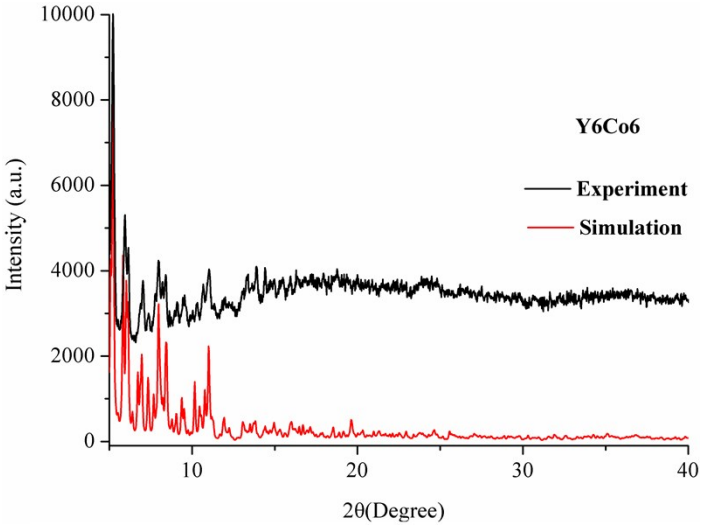

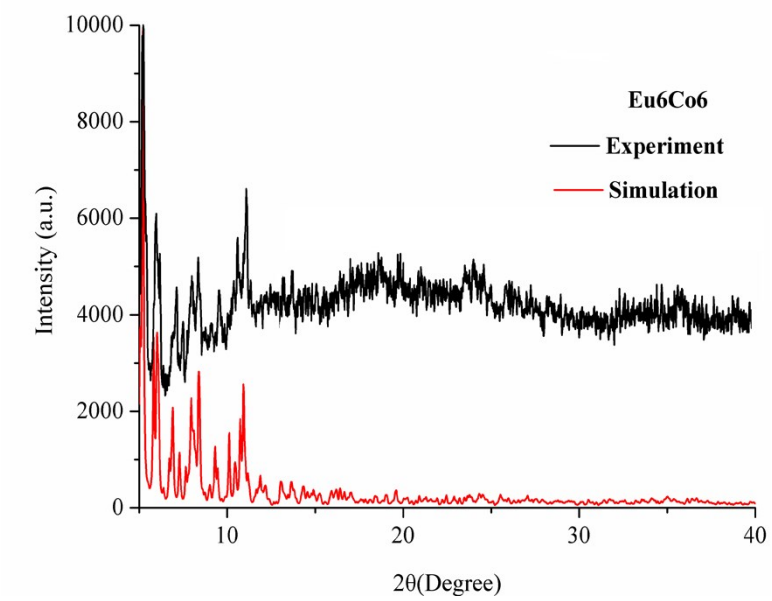

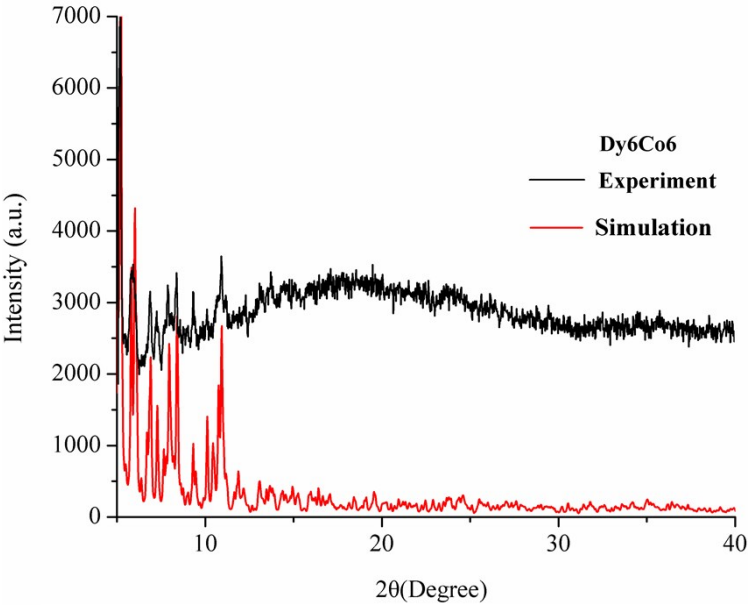

Fig.S5 XRD pattern for compounds **CIAC-248--250.**

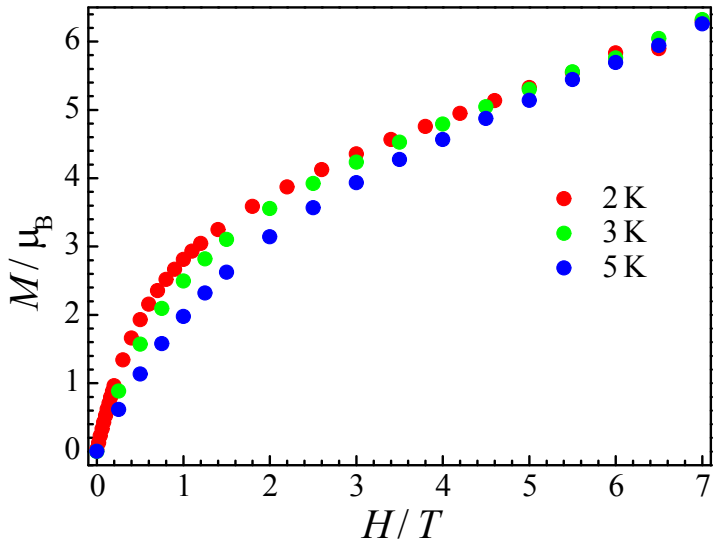

Fig. S6 The field-dependent magnetization plots at indicated temperatures for **CIAC-248**. Lines are visual guide only.

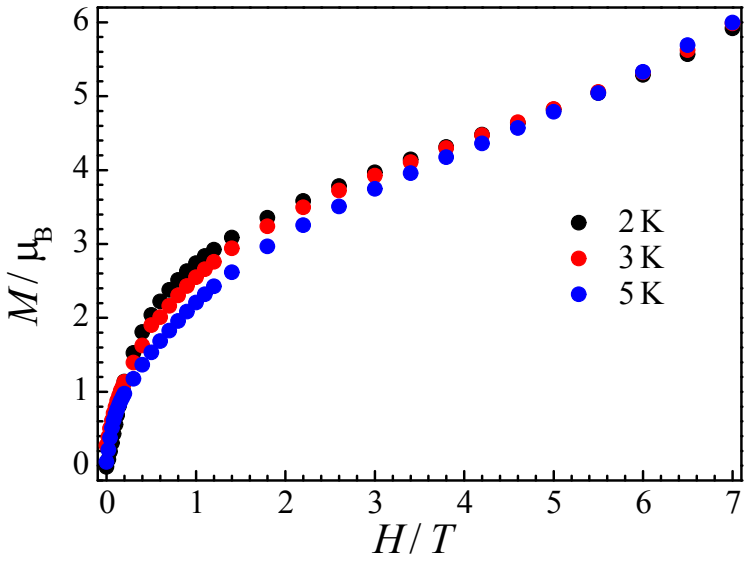

Fig. S7 The field-dependent magnetization plots at indicated temperatures for **CIAC-249**. Lines are visual guide only.

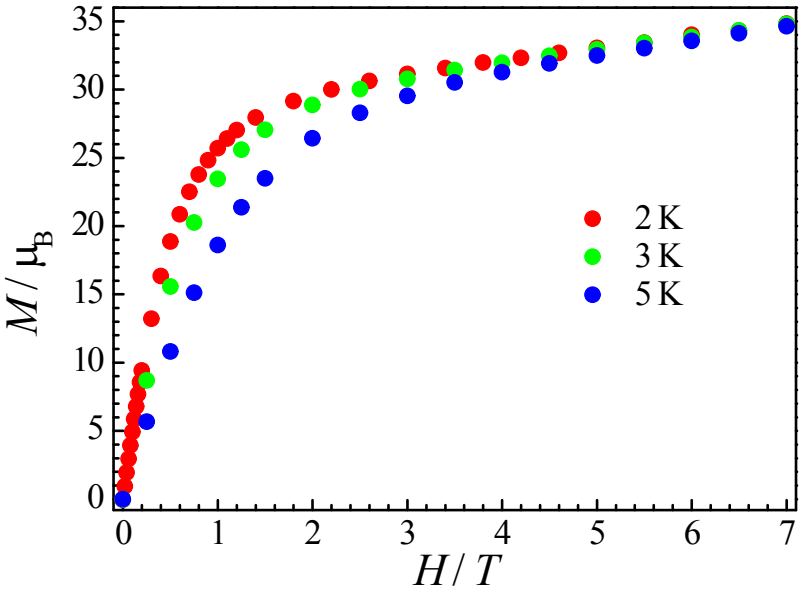

Fig. S8 The field-dependent magnetization plots at indicated temperatures for **CIAC-250**. Lines are visual guide only.

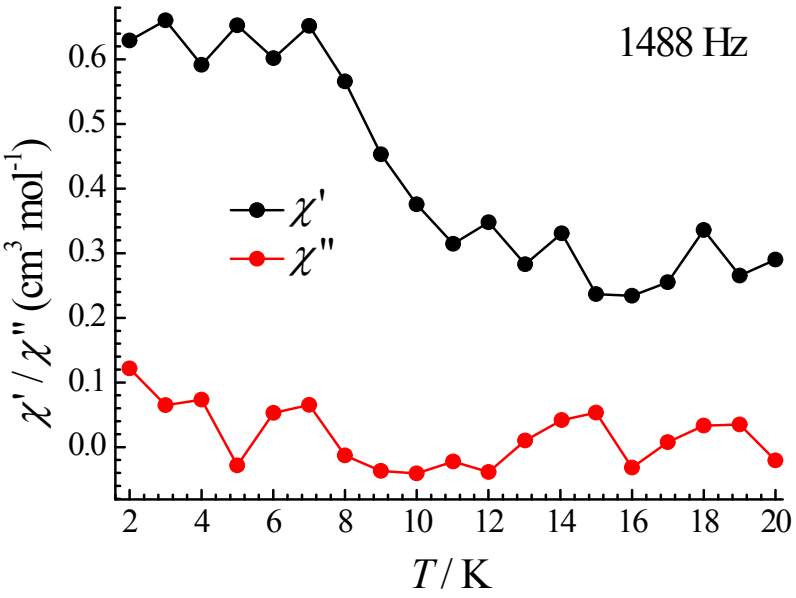

Fig. S9 Temperature-dependence of the in-phase (χ') and out-of-phase (χ'') ac susceptibility signals under zero dc field at the frequency of 1488 Hz for **CIAC-248.**

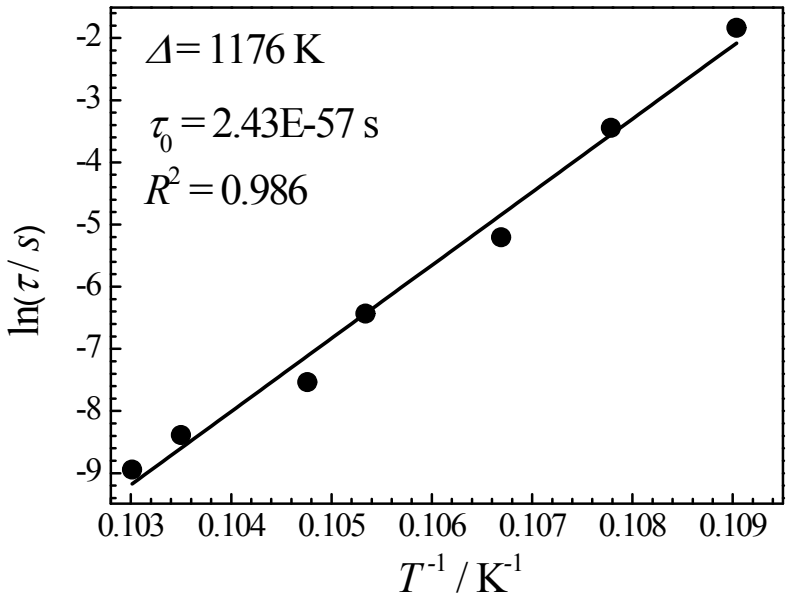

Fig. S10 Plot of ln(τ) versus 1/T for **CIAC-249**. The solid line is the best fit.

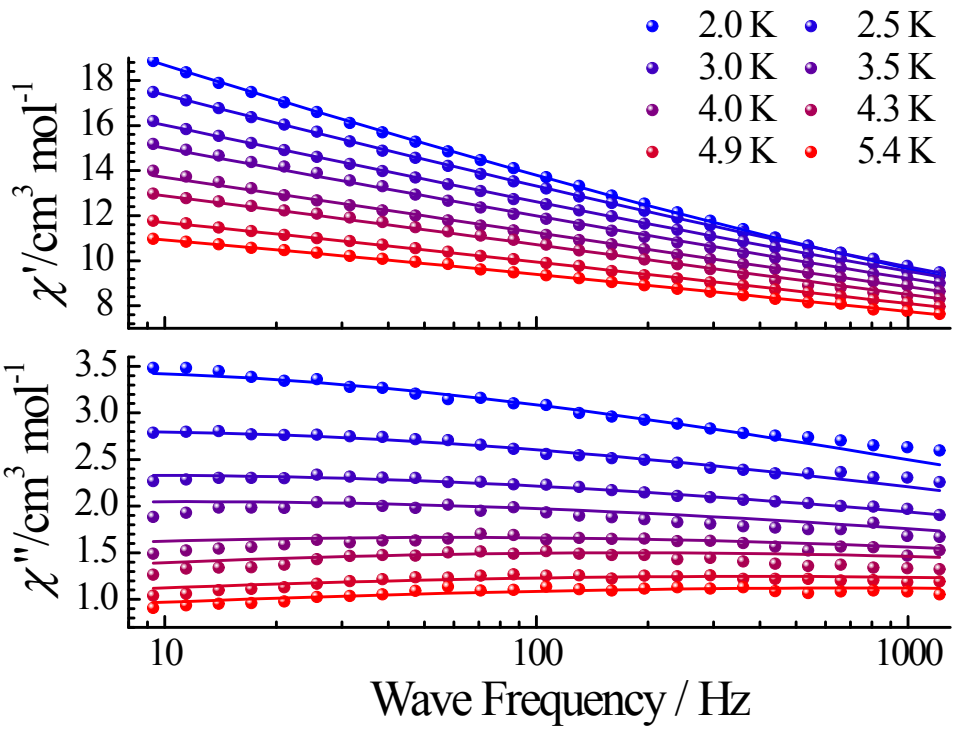

Figure S11 Frequency-dependence of the in-phase (χ') and out-of-phase (χ'') ac susceptibility signals under zero dc field at the indicated temperatures for **CIAC-250**. The solid lines are the best fits.

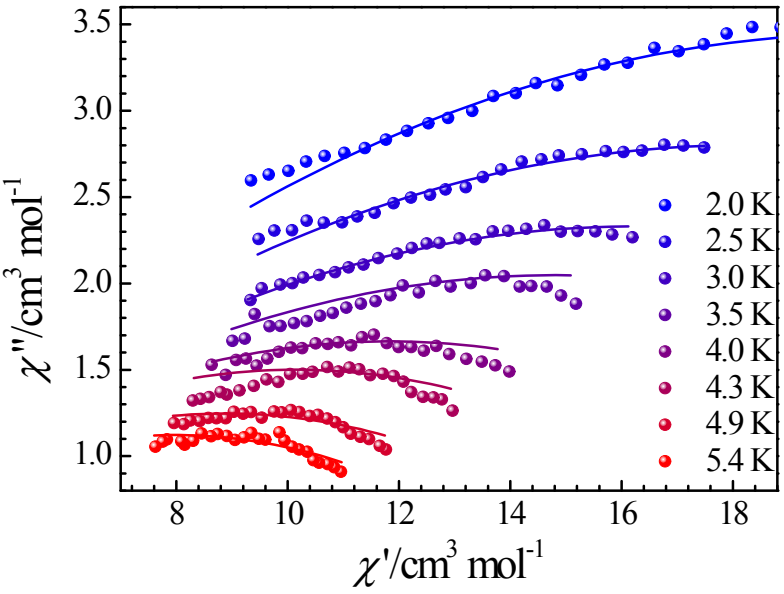

Fig. S12 Cole-Cole plots using the frequency-dependence ac susceptibility data under zero dc field for **CIAC-250**. The solid lines are the best fits.

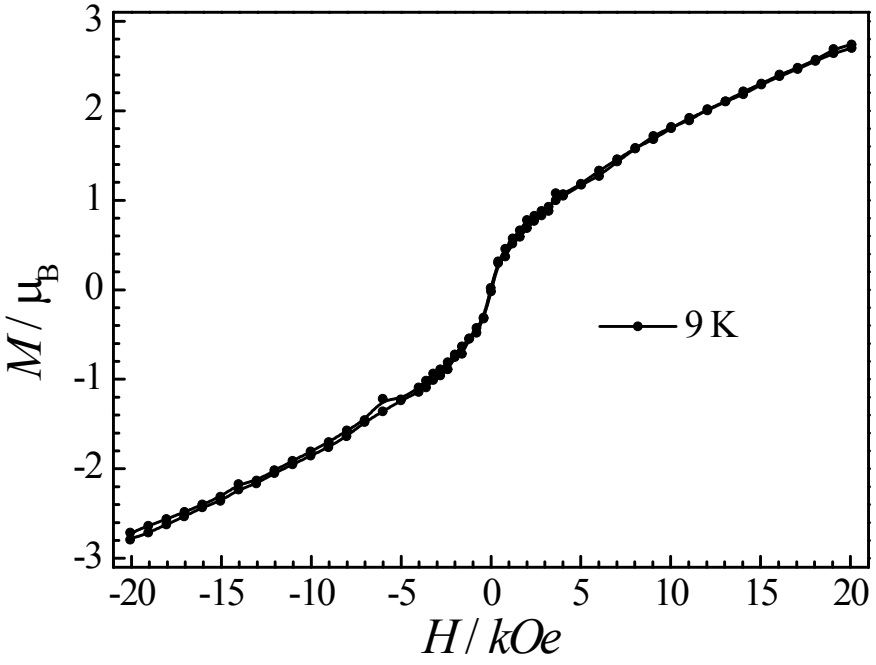

Fig. S13 Magnetic hysteresis measurements for **CIAC-249** with an average sweep rate of 1.2 mT s^{-1}.